Supporting Information

Nitrogen-Enriched Precursor Lowers Debromination Temperature for Solid-State Polymerization into High-Performance Lithium Storage Electrodes

Yang Yang[a], Jinshu Zhang[a], Yantuo Li[a,b], Mingyi Ning[a], Jianxue Wu[a], Bingjie Ma[a], Lexian Liu[a], Wei Liu[a,b*]

[a]
School of Physics, Key Laboratory of Quantum Materials and Devices of Ministry of Education, Frontiers Science Center for Mobile Information Communication and Security
Southeast University
Nanjing 211111, China

[b]
Purple Mountain Laboratories
Nanjing 211111, China

*Corresponding email address: 101012931@seu.edu.cn

Synthesis of 3TBEN.

2,9-Dibromo-1,10-phenanthroline-5,6-dione and benzene-1,2,4,5-tetramine tetrahydrochloride were purchased from Leyan and Aladdin, respectively. 2,9-dibromo-1,10-phenanthroline-5,6-dione (0.77 g, 2.1 mmol), and benzene-1,2,4,5-tetramine tetrahydrochlorid (0.28 g, 1.0 mmol) were transferred into a round bottom flask and suspended in 6 ml of ethanol and 20 ml of acetic acid to make a brown suspension in an Ar atmosphere with stirring, and heated to 100 °C. After the addition of 1.0 ml of triethylamine, the mixture immediately changed to a red color, and was further refluxed at 130 °C for 6 h. Once cooled to room temperature the mixture was diluted with acetic acid and poured into 200 ml of water. The red precipitate was collected and exhaustively washed by Soxhlet extraction with water, ethanol, N,N-dimethylformamide and ethanol again, and dried at 120 °C overnight to yield 3TBEN as brown powder (yield: ~69%). High-resolution MS (negative mode) m/z = 803.2956 (calcd. 803.7701); 1H NMR (300 MHz, CF3COOD-d): d 10.33 (s, J=2.1 Hz, 4H), 9.85 (s, J=2.1 Hz, 2H), 9.39 (s, J=2.1 Hz, 4H)

Thermal-initiated endogenous solid-state polymerization.

The polymerization of 3TBEN was performed in a tube furnace under an Ar atmosphere. The 3TBEN powder was heated from room temperature to 480 °C and maintained at 480 °C for 300 minutes to complete the solid-state polymerization process. The obtained product was used for characterization without further purification.

Materials characterizations

^{1}H NMR spectra were recorded on a Bruker AVANCE 300 MHz NMR spectrometer using trifluoroacetic acid (TFA) as the solvent. High-resolution mass spectra (HRMS) were recorded on a Thermo Fisher Scientific Q Exactive Plus mass spectrometer operated in the negative ion mode using an atmospheric pressure chemical ionization (APCI) source. The morphology of 8N-CAP was examined using scanning electron microscopy (SEM) with FEI Inspect F50 Microscope. CO_2 sorption isotherms were measured at 273K with Quantachrome IQ, and pore size distributions were calculated by the Density Functional Theory (DFT) method. Fourier-transform infrared spectroscopy (FTIR) was performed with an IR Tracer-100 spectrometer. X-ray photoelectron spectroscopy (XPS) data were collected with an ESCALAB 250 XI (Thermo Kalpha) equipped with mono Al Kα. Raman spectra were determined by Horiba Jobin Yvon, XploRA Plus.

Coin cells assembly and electrochemical performance measurements

Electrochemical measurements of half-cells were conducted using CR2032 coin cells at 25 °C. All cells were assembled in an argon-filled glove box, with the H_2O and O_2 levels below 0.1 ppm. Charge-discharge tests were performed using the NEWARE test system at various current densities within a voltage window of 0.01 to 3.00 V versus Li^+/Li at room temperature. Cyclic voltammetry (CV) measurements were carried out using an electrochemical workstation (Chenhua Instrument, CHI760E). Lithium tablets were employed as reference and counter electrodes, and glass fiber was used as the separator. The working electrodes were prepared by mixing 8N-CAP polymer, Super P, and sodium alginate binder in a mass ratio of 6: 3: 1 with water. The mixture was stirred for 12 hours

to form a uniform slurry, which was then coated onto Cu foil and vacuum dried at 120 °C overnight. The mass loading of 8N-CAP on each anode was approximately 1 mg cm^{-2} The electrolyte consisted of 1 M LiPF6 in a 1:1 (v/v) mixture of ethylene carbonate (EC) and dimethyl carbonate (DMC). For evaluation of the Na storage capability, sodium metal was used as counter electrode and 1.0 M $NaPF_6$ in DME was employed as electrolyte.

Diffusion coefficient (D) is calculated based on Fick's second law using:

$$D = \frac{4}{\Pi}\left(\frac{n_m}{F}\right)^2\left(\frac{I}{A}\right)^2\left(\frac{\tau}{(\Delta E/\Delta Es)^2}\right)$$

n_m is the number of lithium ions in the material.

F is the Faraday constant.

I is the applied constant current.

A is the area of the electrode.

τ is the duration of the current pulse.

$\Delta E\tau$ is the voltage change during the current pulse.

ΔEs is the steady-state open-circuit voltage change.

Density functional theory (DFT) calculations

Density functional theory (DFT) calculations were performed using the Vienna ab initio Simulation Package (VASP). The projected augmented wave (PAW) method and Perdew-Burke-Ernzerhof (PBE) functional were used to describe the interaction between the ion-core and valence electron and the exchange-correlation(xc) interaction, respectively. For computational procedures, Brillouin zone integration was implemented with 2 x 2 x 1 Gamma-centre k-point sampling. A plane wave cutoff energy of 500 eV was used for total energy calculations, where the force convergence and the electronic self-consistent convergence were set to 0.02 eV/A and 1 x 10-6 eV/atom, respectively. The van der Waals（vdW） interaction was treated using the DFT-D3 method. To suppress the interlayer interaction caused by periodic boundary conditions, a vacuum layer of 15 Å was introduced in the calculations.

Supporting Figures

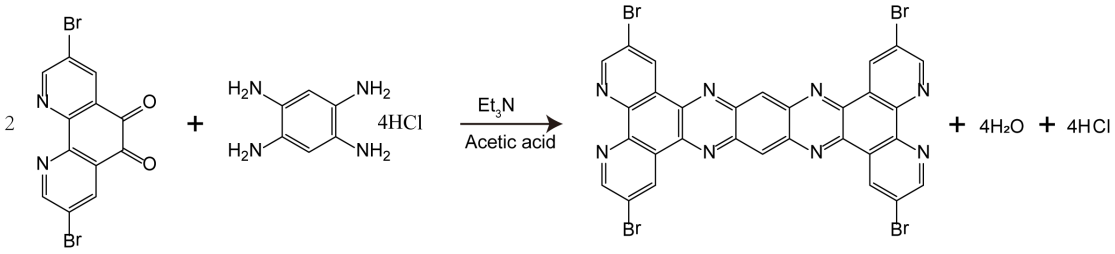

Fig. S1 Molecular design of 3TBEN.

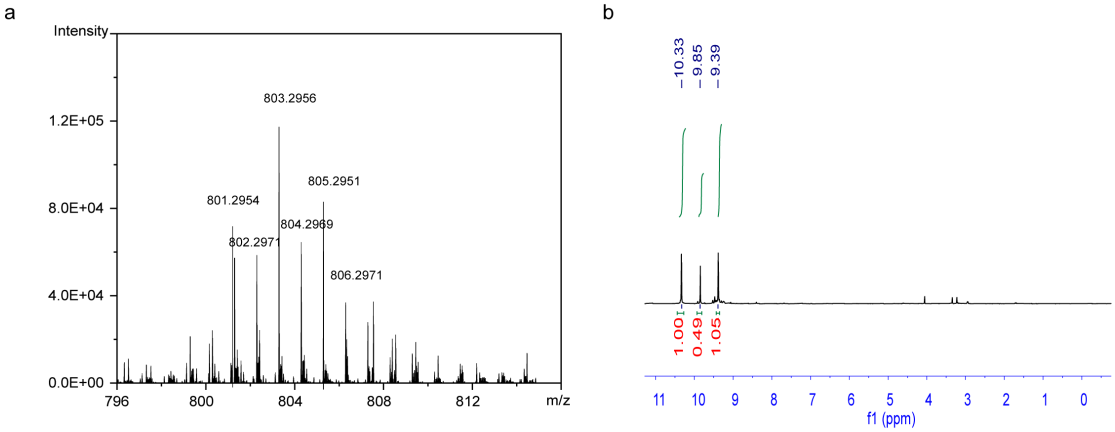

Figure. S2 (a) High-resolution mass spectrum of 3TBEN. (b) 1H NMR spectrum of 3TBEN in TFA-d_1.

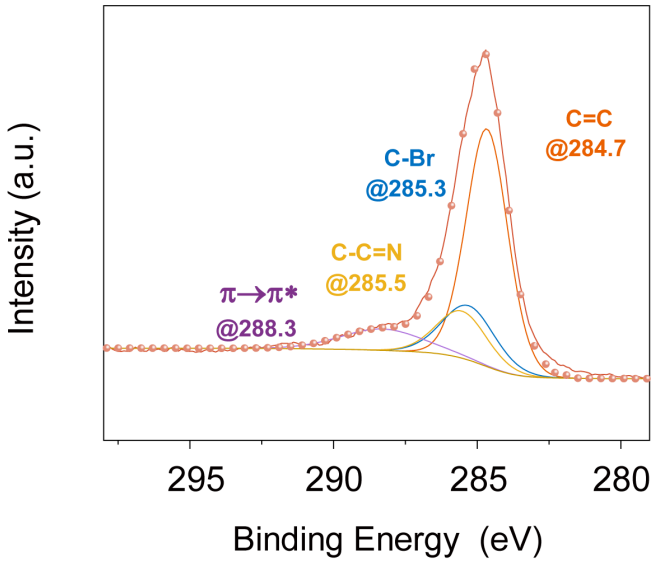

Fig. S3 C1s XPS spectrum of 3TBEN.

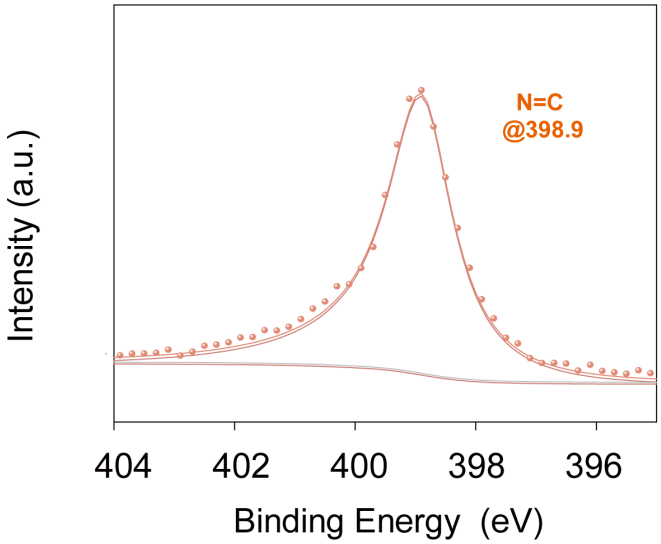

Fig. S4 N1s XPS spectrum of 3TBEN.

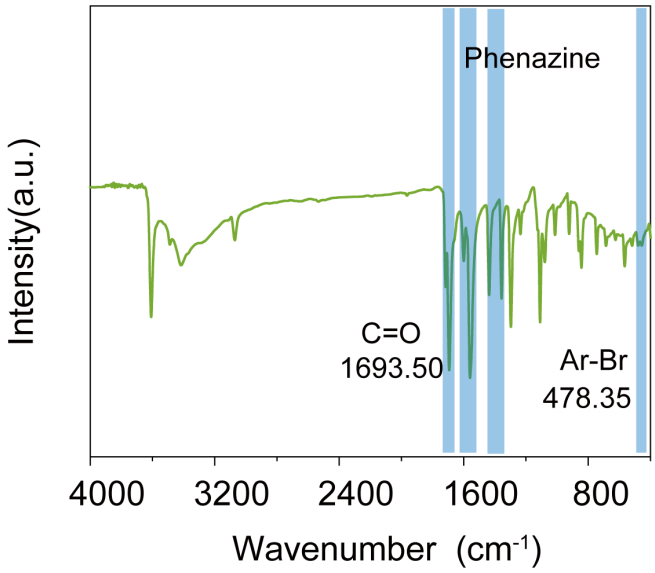

Fig. S5 FTIR spectrum of 2,9-Dibromo-1,10-phenanthroline-5,6-dione

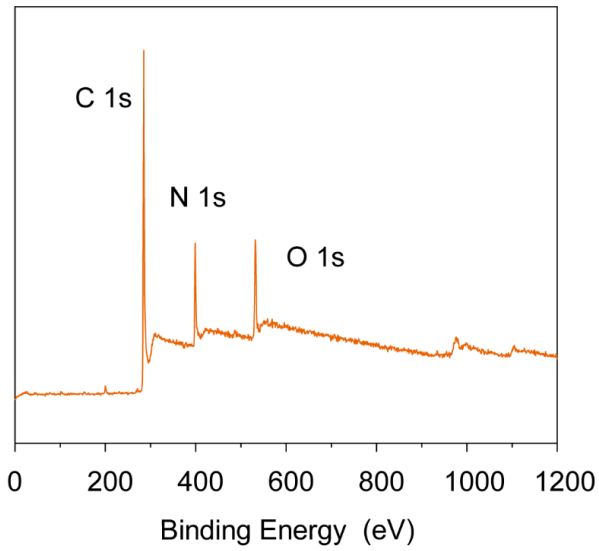

Fig. S6 XPS spectrum of 8N-CAP.

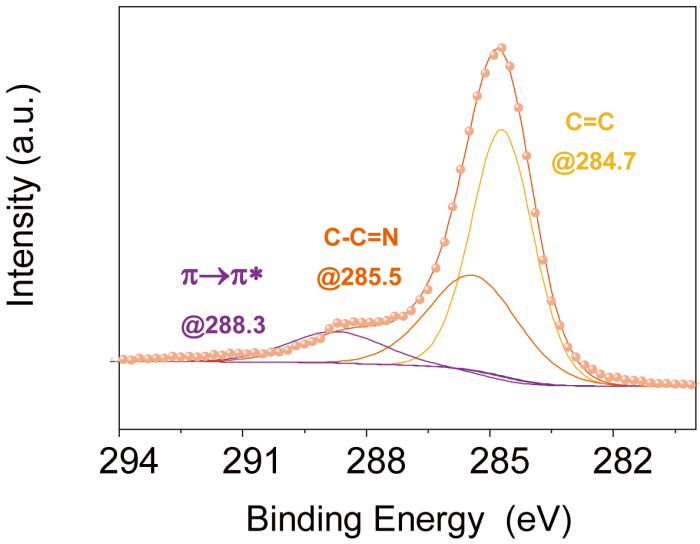

Fig. S7 C1s XPS spectrum of 8N-CAP.

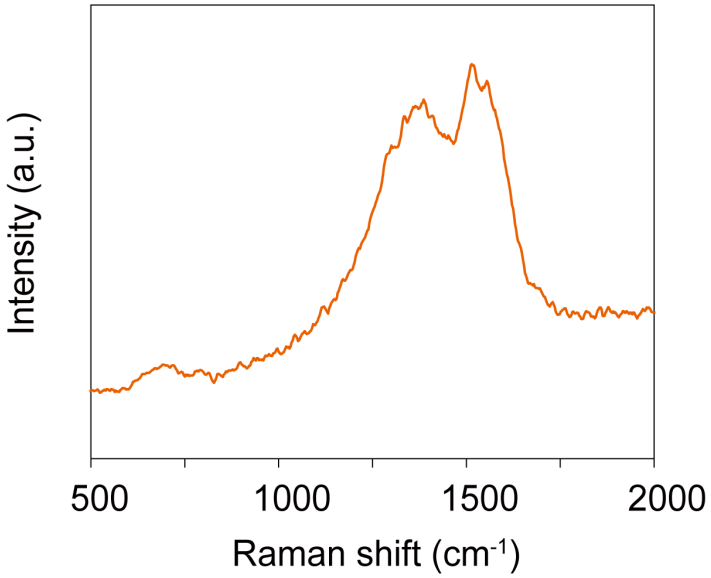

Fig. S8 Raman spectrum of 8N-CAP.

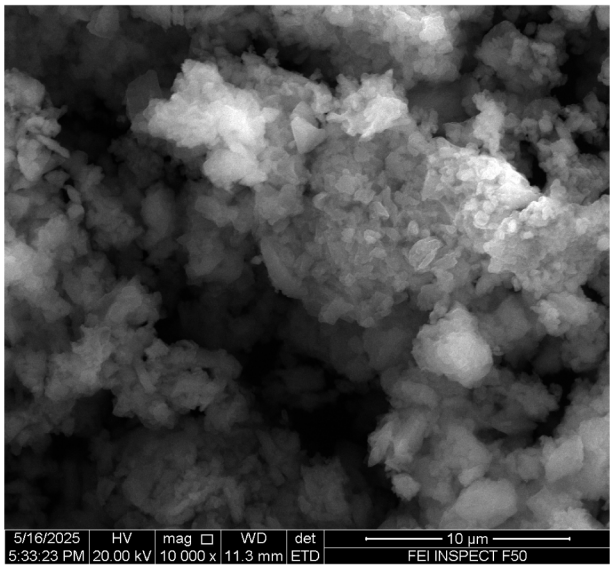

Fig. S9 SEM image of 8N-CAP.

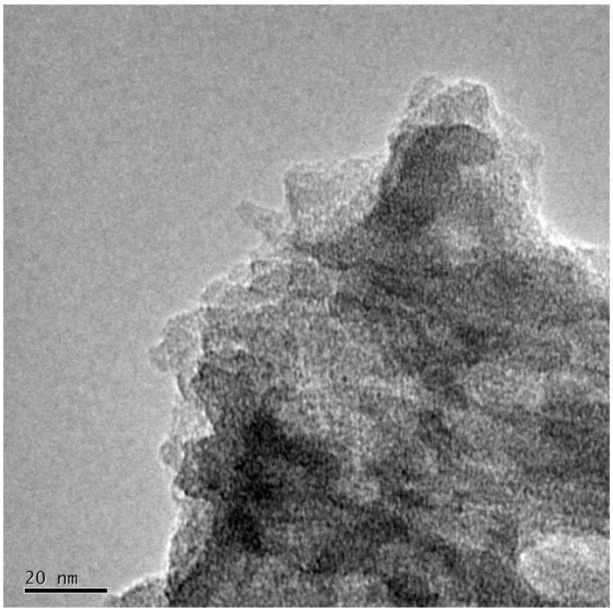

Fig. S10 TEM image of 8N-CAP.

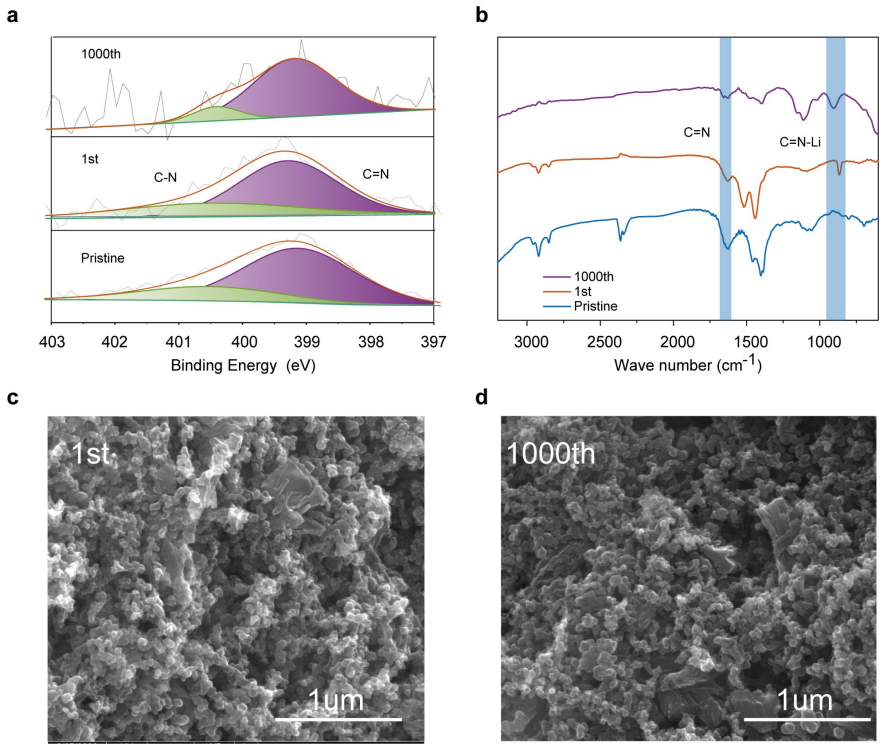

Fig. S11 Post-cycling characterization of the electrode. (a) N 1s XPS spectra of the pristine, 1st-cycled, and 1000th-cycled electrodes.(b) FTIR spectra of electrodes during cycling. (c) SEM image after the 1st cycle. (d) SEM image after the 1000th cycle.

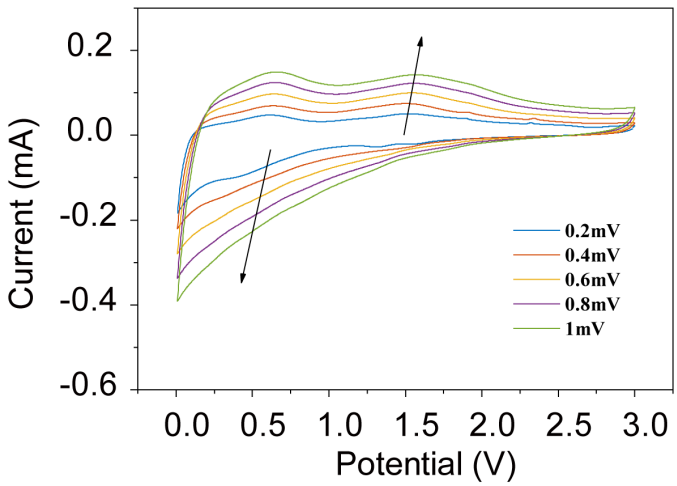

Fig. S12 CV curves of 8N-CAP at various scan rates from 0.2 to 1.0 mV s^{-1}

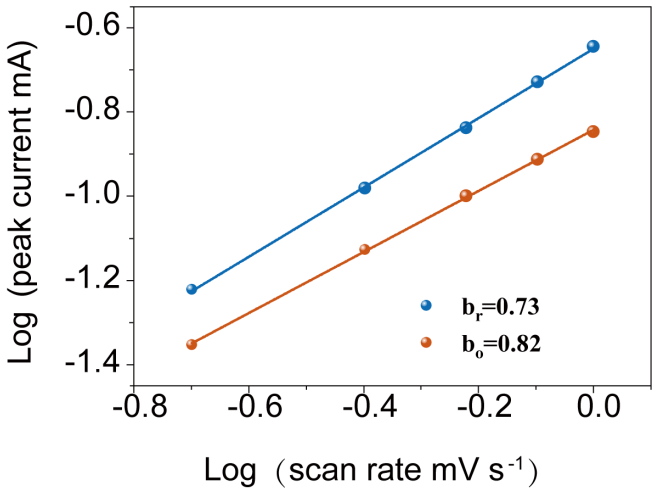

Fig. S13 Corresponding linear fits of the peak current of CV curves of 8N-CAP.

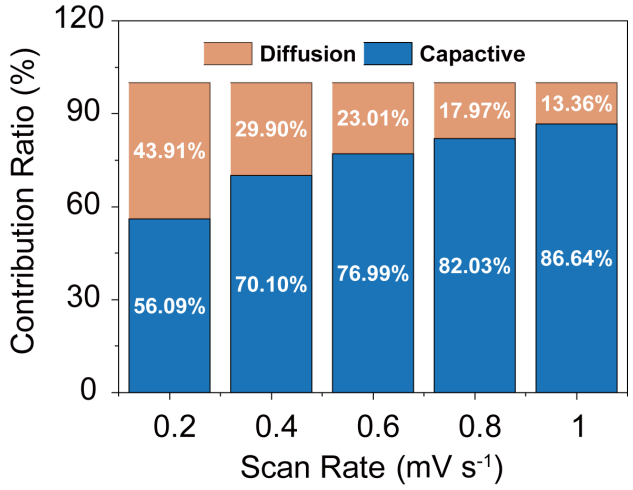

Fig. S14 The pseudocapacitive and diffusion-controlled charge storage contributions at different scan rates of 8N-CAP.

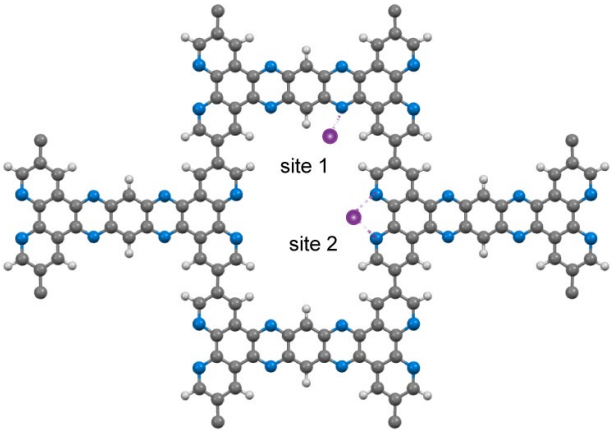

Fig. S15 Schematic illustration of the Li^+ binding sites used for binding energy calculations.

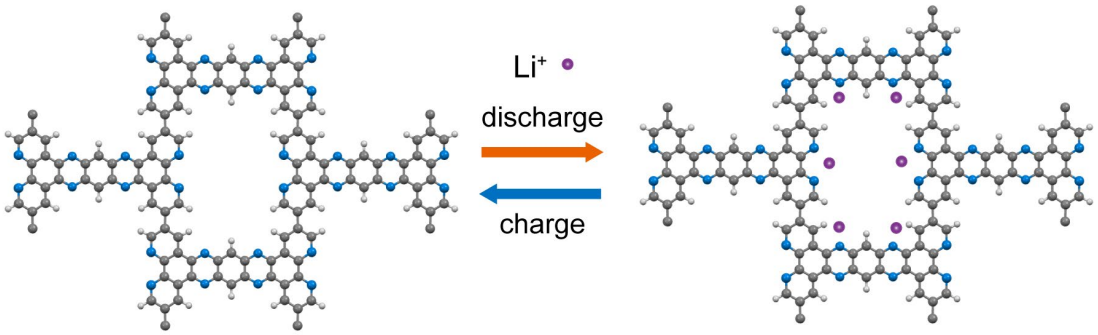

Fig. S16 Schematic illustration of the lithium-storage process in 8N-CAP.

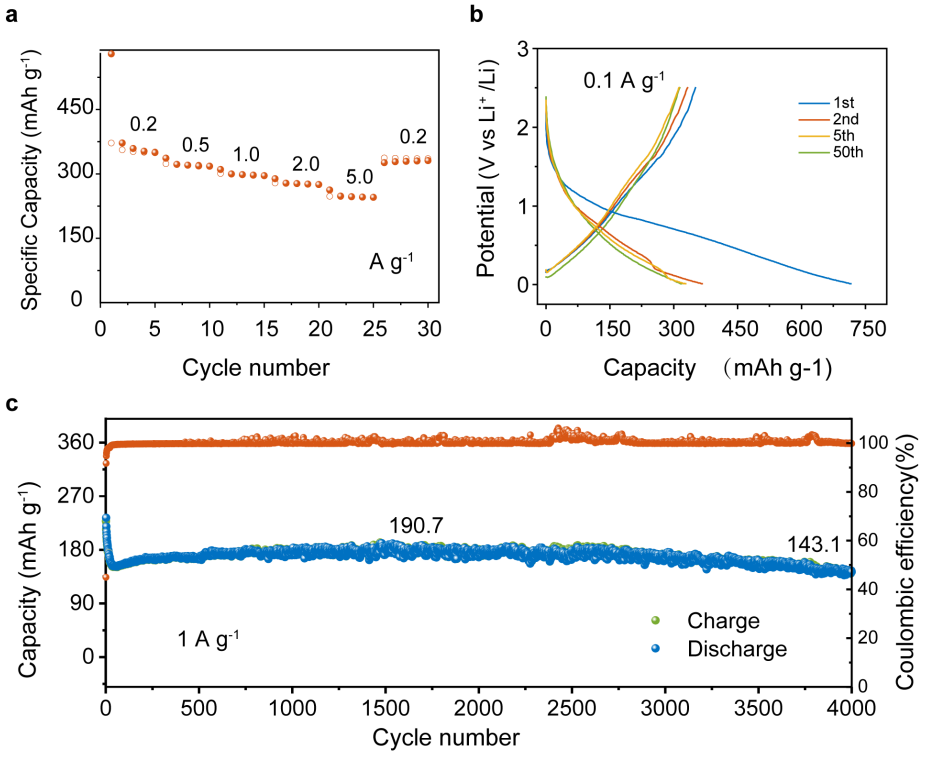

Fig. S17 Electrochemical performance of 8N-CAP as sodium ion storage anodes. (a) Rate performance of 8N-CAP. (b) Galvanostatic charge–discharge profiles of 3TBEN at 0.1 A g^{-1}. (c) Long-term cycling performance of 8N-CAP at 1 A g^{-1}.

The sodium storage performance of 8N-CAP was evaluated using Na-ion half cells with sodium metal as the counter electrode. The rate capability (a) evaluated at current densities of 0.2, 0.5, 1.0, 2.0 and 5.0 A g^{-1} shows corresponding capacities of roughly 350, 312, 290, 273, and 245 mA h g^{-1}, respectively. When the current is returned to 0.2 A g^{-1}, the capacity recovers to ~322 mA h g^{-1}, demonstrating excellent rate performance and structural robustness. At 1.0 A g^{-1}, the electrode maintains a stable reversible capacity of ~197 mA h g^{-1} after 10 cycles, and retains~143 mA h g^{-1} over 4000 cycles (c), highlighting its superior long-term cycling stability.

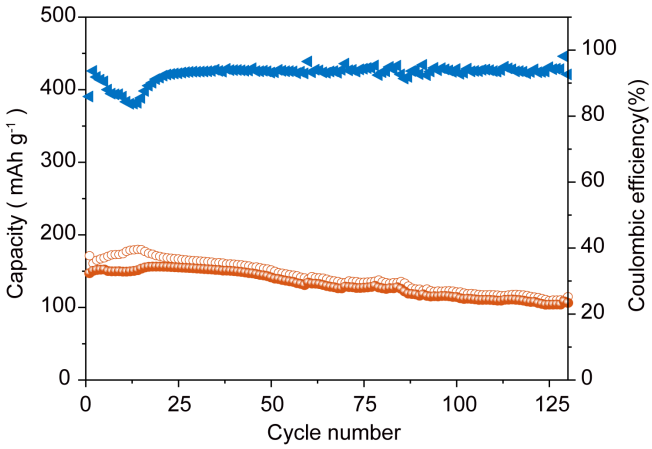

Fig. S18 Cycling performance and the corresponding Coulombic efficiency of the fabricated full cell.

Electrochemical test of the full cell was carried out using a 2032 type coin cell with 8N-CAP material as the anode, $LiFePO_4$ as the cathode, and a 1 M LiPF6 EC:DMC 1:1 solution as the electrolyte. Prior to cell testing, the anode was activated according to Fahlman's research [1]. The full cell was cycled at 85 mA g^{-1} ($LiFePO_4$ as calibration), which is about 300 mA g^{-1} calibrated to 8N-CAP, within a 1.5-4.2 V voltage limit. Fig. S18 shows the cycling response of the full cell. The first discharge and charge capacities are 171.3 and 141.2 mA h g^{-1}, respectively, and a discharge capacity of ~120 mA h g^{-1} after 120 cycles.

References

1. J. Chen, Z. Mao, L. Zhang, D. Wang, R. Xu, L. Bie and B. D. Fahlman, ACS Nano, 2017, **11**, 12650 – 12657.